Johann Radon Institute for
Computational and Applied Mathematics
Austrian Academy of Sciences (ÖAW)

Multilevel preconditioning in $H(\mathrm{div})$ and applications to a posteriori error estimates for discontinuous Galerkin approximations

J. Kraus, S. Tomar

RICAM-Report 2008-30

MULTILEVEL PRECONDITIONING IN $H(\mathrm{DIV})$ AND APPLICATIONS TO A POSTERIORI ERROR ESTIMATES FOR DISCONTINUOUS GALERKIN APPROXIMATIONS

J. K. KRAUS[†] AND S. K. TOMAR[†]

Abstract. An optimal order algebraic multilevel iterative (AMLI) method for solving systems of linear algebraic equations arising from the finite element discretization of certain boundary value problems, that have their weak formulation in the space $H(\mathrm{div})$, is presented. The algorithm is used for the solution of the discrete minimization problem which arises in the functional-type a posteriori error estimates for the discontinuous Galerkin (DG) approximation of elliptic problems. The method is theoretically analyzed and supporting numerical examples are presented. By comparing the computing time for the proposed solver and the AMLI solver for the DG problem it is shown that the *guaranteed and sharp* error bounds can be computed with a reasonable cost.

Key words. Algebraic multilevel iteration; a posteriori error estimates; (discontinuous Galerkin) finite element discretization; lowest order Raviart-Thomas space

AMS subject classifications. 65N30, 65N22, 65N55

1. Introduction.

A posteriori error estimates for conforming finite element approximations of various boundary value problems, starting with the foundational work of Babuska and Rheinboldt [11], have been extensively studied and a huge literature devoted to this topic can be found. For brevity reasons we refer here only some of the books [2, 12, 13, 36, 49] and the references therein. A posteriori error estimates for discontinuous Galerkin (DG) approximations, on the other hand, have gained significant interest only in recent years, particularly, because the DG methods, after their introduction in the late 70s, were lying almost dormant till the early 90s. For some of the articles on a posteriori error estimates for DG methods applied to elliptic problems see, e.g., [1, 15, 28, 29, 30, 44, 47]. The underlying ideas of the majority of these a posteriori error estimates are either the analysis of the residuals (explicit/implicit), post-processing (superconvergence phenomena, equilibrated fluxes), or adoint problems (goal-oriented). In general, these estimates may perform as a good indicator, however, the respective bounds lack the *sharpness*. Moreover, they require additional assumptions, e.g. Galerkin orthogonality or extra regularity for sharpness. In fact, the computed upper bounds obtained from these methods may be several orders larger in magnitude than the true error [19, 20]. Following the important work of Repin [38, 39, 40, 41, 42], see [36] for a systematic exposition, a new approach towards a posteriori error estimates has been initiated where the emphasis is on the *guarantee, computability (without unknown constants) and sharpness* of the bounds. These so-called *functional* a posteriori estimates, which give *guaranteed, computable, and sharp* upper and lower bounds of the error in the energy norm, are derived on purely functional grounds by the analysis of the respective differential problem, and therefore, they are valid for *any conforming approximation* of the exact solution. In general, because the error of the DG approximations is not in the natural energy space $H^1(\Omega)$, the treatment of the overall error usually consists of decomposing it into two terms (see e.g., [1, 23, 30]), a nonconforming part and a conforming part. Since the nonconforming part can be computed explicitly, this essentially leads to the derivation of the upper (lower) bounds for the conforming part. Using this decomposition and the triangle inequality *guaranteed and sharp* a posteriori error estimates for DG approximations of elliptic problems have been proposed in [35, 48]. Since the nonconforming error, which can be viewed as a *penalty for the nonconformity*, is explicitly determined, these estimates are also valid for any nonconforming

[†]Johann Radon Institute for Computational and Applied Mathematics, Austrian Academy of Sciences, Altenbergerstrasse 69, A-4040 Linz, Austria. ({johannes.kraus,satyendra.tomar}@oeaw.ac.at)

(DG) approximation. In a very recent work [23] Ern et. al. have also proposed guaranteed and robust a posteriori error estimates for DG approximations, which are based on the flux reconstruction.

As noted in [35, 48], for sharp bounds in these functional a posteriori error estimates it is required to solve a system of linear algebraic equations for a vector-valued function in the space $H(\Omega, \mathrm{div})$. This process is not cheap, in fact, its cost could be more than the cost of finding the DG solution for difficult problems. This necessitates the development of fast iterative solution techniques for problems in $H(\Omega, \mathrm{div})$. Preconditioning methods for such linear systems within the framework of domain decomposition and multigrid techniques have been studied by several authors, see e.g., [5, 6, 26]. In this article we develop optimal order iterative solvers for problems in the space $H(\Omega, \mathrm{div})$ within the framework of algebraic multilevel iteration (AMLI) methods, and extend their applicability and analysis to discretizations of minimization problems related to a posteriori error estimates . Note that, apart from the said interest in a posteriori error estimates, such iterative schemes are also important for an efficient numerical solution of practical problems, e.g., in continuum mechanics. The AMLI methods, which were originally presented in [8, 9], are recursive extensions of two-level FE methods that themselves have been introduced and extensively analyzed in the context of conforming methods, see e.g., [7, 8, 9, 14]. A peculiarity in the AMLI method is to use certain stabilization techniques in order to make the overall iterative solution process of optimal order of computational complexity. The stabilization of the condition number can be achieved by employing a properly shifted and scaled Chebyshev polynomial in each coarse-level update, see [8, 9]. Alternatively, inner iterations at all (or at certain) coarse levels can be used to stabilize the outer iteration [10, 31, 37]. Recently, such AMLI-type solvers have also been studied and analyzed in the context of nonconforming methods, see [16, 24, 32], and DG approximations [33, 34].

The remainder of the paper is organized as follows. Section 2 deals with preliminaries on DG approximations of elliptic boundary-value problems. In Section 3 we briefly recall the a posteriori error estimates for DG approximations of elliptic problems from [35, 48]. We then discuss the discrete formulation of the minimization problem, which results from the a posteriori error estimates, by the lowest-order Raviart-Thomas elements. The main results of this paper follow in Section 4 which contains new recursive estimates for the constant in the strengthened Cauchy-Bunyakowski-Schwarz (CBS) inequality, the latter being of fundamental importance in the classical AMLI convergence theory [8, 9]. In Section 5 we present some numerical experiments that illustrate the theoretical results and demonstrate the reasonable cost of solving the linear systems arising from the sharp a posteriori error estimates by relating it to the cost of computing the DG approximation. Finally, concluding remarks are presented in Section 6.

2. Preliminaries. We consider a second order elliptic problem on a bounded Lipschitz domain $\Omega \subset \mathbb{R}^2$, with Dirichlet boundary data

$$-\mathrm{div}\ (\underline{A}(x)\nabla u) = f(x) \quad \text{in } \Omega, \quad u(x) = u_0 \quad \text{on } \partial\Omega. \tag{2.1}$$

We assume that $\underline{A}$ is a symmetric positive definite matrix such that

$$c_1|\xi|^2 \le \underline{A}\xi \cdot \xi \le c_2|\xi|^2, \quad \forall \xi \in \mathbb{R}^2, \tag{2.2}$$

and it has a positive inverse $\underline{A}^{-1}$. For the sake of simplicity we restrict ourselves to the Dirichlet boundary data, however, the method is also applicable with mixed boundary data, see [35] for details.

Let $\mathcal{T}_h$ be a non-overlapping partition of Ω into finite elements K (of polygonal or polyhedral shape), with boundaries ∂K. We allow finite elements to vary in size and shape for local

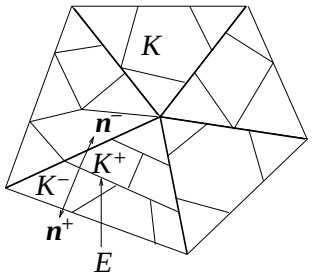

FIG. 2.1. *A possible DG mesh on* Ω

mesh adaptation and the mesh is not required to be conforming, i.e. elements may possess hanging nodes, see Figure 2.1. Let h_K denote the size of the element K and $h = \max_{K\in\mathcal{T}_h} h_K$ denote the characteristic mesh size. We assume that the partition is shape regular [45], i.e., there exist a positive constant κ, independent of h, such that $\sup_{K\in\mathcal{T}_h} \frac{h_K}{\rho_K} \leq \kappa < \infty$, where ρ_K denotes the diameter of the largest circle inscribed in K. This condition means that the elements $K \in \mathcal{T}_h$ do not have arbitrarily small angles. Further, let E be an interior face shared by two adjacent elements K^+, and K^-. We denote the set of all such internal faces by $\mathcal{E}_0$, the set of faces on $\partial\Omega$ by $\mathcal{E}_D$, and the set of all faces by $\mathcal{E} : \mathcal{E} = \mathcal{E}_0 \cup \mathcal{E}_D$. The face measure h_E is constant on each face $E \in \mathcal{E}$ such that $h_E = |E|$.

We now define the space

$$\mathcal{V}_0 := H^1_D(\Omega) = \{v \in H^1(\Omega) \ : \ v|_{\partial\Omega} = u_0\},$$

where $H^1(\Omega)$ is the usual Sobolev space. We also define the space of polynomials

$$P_{k_1,k_2}(K) = \left\{p(x,y) \mid p(x,y) = \sum_{i\leq k_1, j\leq k_2} a_{i,j} x^i y^j\right\}.$$

We then define the space of polynomials of degree $\leq r$ in both the variables x and y

$$Q_r(K) = P_{r,r}(K).$$

Further, on the partition $\mathcal{T}_h$ we define the finite dimensional space:

$$\mathcal{V}_h = \{v \in L^2(\Omega) \ : \ v|_K \in Q_r(K), \ r \geq 1, \ \forall K \in \mathcal{T}_h\}.$$

Note that on $\mathcal{V}_h$ neither any boundary condition nor any inter-element continuity is enforced. The inter-element continuity will be enforced indirectly via the variational formulation. We shall also need the following space in the sequel

$$H(\Omega, \mathrm{div}) = \{\boldsymbol{v} \in (L^2(\Omega))^2, \ \mathrm{div}\, \boldsymbol{v} \in L^2(\Omega)\}.$$

To deal with the multivalued traces at the inter-element faces we define the trace operators $\{\cdot\}$ and $[\![\cdot]\!]$, `average` and `jump`, respectively, as follows [4]: Let $E \in \mathcal{E}_0$. Define the unit normal vectors $\boldsymbol{n}^+$ and $\boldsymbol{n}^-$ on E pointing exterior to K^+ and K^-, respectively. For $v \in \mathcal{V}_h$ we define $v^{+/-} := v|_{\partial K^{+/-}}$ and set

$$\{v\} = \frac{1}{2}(v^+ + v^-), \quad [\![v]\!] = v^+\boldsymbol{n}^+ + v^-\boldsymbol{n}^-, \quad \text{on } E \in \mathcal{E}_0.$$

On $E \in \mathcal{E}_D$ the traces are uniquely defined and are set as

$$\{v\} = v, \quad [\![v]\!] = v\boldsymbol{n}.$$

Now, we define the following inner-product norms on $H^1(\Omega)$

$$\|v\|_a^2 = \int_\Omega \underline{A} v \cdot v \, dx, \quad \|v\|_{\tilde{a}}^2 = \int_\Omega \underline{A}^{-1} v \cdot v \, dx. \tag{2.3}$$

Together with (2.2) these norms are equivalent to the L^2 norm on Ω, i.e. $\|v\|_\Omega$. Finally, on $\mathcal{V}_h$ we define the following weighted broken (DG) norm:

$$|[\![v_h]\!]|^2 = \sum_{K\in\mathcal{T}_h} \int_K \underline{A}\nabla_h v_h \cdot \nabla_h v_h \, dx + \eta h_E^{-1} \sum_{E\in\mathcal{E}} \int_E [\![v_h]\!] \cdot [\![v_h]\!] \, ds, \tag{2.4}$$

where η is the stabilization parameter of the symmetric interior-penalty (IP) discontinuous Galerkin (DG) method and has to be sufficiently large to guarantee the coercivity of the discrete bilinear form [4, 22].

For the sake of completeness we provide here the DG formulation. For elliptic boundary value problems a large number of DG methods have been developed, see e.g. [4, 17] and the references therein. In this article we consider the interior-penalty (IP) DG method. For the problem (2.1) the IP-DG formulation can be stated as follows:
Find $u_h \in \mathcal{V}_h$ such that for all $v_h \in \mathcal{V}_h$ the following relation holds:

$$\mathcal{B}_h(u_h, v_h) = \mathcal{L}_h(v_h), \tag{2.5a}$$

where the bilinear form $\mathcal{B}_h(u_h, v_h) : \mathcal{V}_h \times \mathcal{V}_h \to \mathbb{R}$ and the linear form $\mathcal{L}_h(v_h) : \mathcal{V}_h \to \mathbb{R}$ are defined as

$$\begin{aligned}\mathcal{B}_h(u_h, v_h) = &\sum_{K\in\mathcal{T}_h} \int_K \underline{A}\nabla_h u_h \cdot \nabla_h v_h \, dx + \eta h_E^{-1} \sum_{E\in\mathcal{E}} \int_E [\![u_h]\!] \cdot [\![v_h]\!] \, ds \\ &- \sum_{E\in\mathcal{E}} \int_E (\{\underline{A}\nabla_h u_h\} \cdot [\![v_h]\!] + [\![u_h]\!] \cdot \{\underline{A}\nabla_h v_h\}) \, ds,\end{aligned} \tag{2.5b}$$

$$\mathcal{L}_h(v_h) = \int_\Omega f v_h \, dx. \tag{2.5c}$$

The bilinear form $\mathcal{B}_h$ is coercive and bounded in $\mathcal{V}_h$, equipped with the norm (2.4), for $\eta > 0$ sufficiently large, see e.g. [4, 22]. Further, for $f \in L^2(\Omega)$ the problem (2.5) has a unique solution $u_h \in \mathcal{V}_h$. The IP-DG method delivers an optimal order of convergence in the DG norm (2.4) as well as, when equipped with elliptic regularity, in the L^2 norm. For proofs see, e.g., [4].

REMARK 2.1. *For a posteriori error estimates we do not need any specific structure of the DG schemes and instead of the IP-DG method we can use any of the DG methods found in the literature [4, 17].*

3. A posteriori error estimates and the discrete formulation. Let $\tilde{u}_h$ denote a conforming approximation obtained from u_h such that the *nonconforming* error $\tilde{u}_h - u_h$ is minimal. One such cheap method is based on the Oswald interpolation operator, see e.g. [23, 29, 48] (another projection can be found in [35]).

From [35, 48] we have the following upper bound of the error in the DG approximation

$$|[\![u - u_h]\!]| \le M_\oplus^{\frac{1}{2}} + |[\![\tilde{u}_h - u_h]\!]|, \tag{3.1}$$

$$\text{where} \quad M_\oplus = (1+\beta)\|\underline{A}\nabla\tilde{u}_h - \boldsymbol{\tau}\|_a^2 + (1 + 1/\beta)C_{\Omega,\underline{A}}^2 \|\operatorname{div}\boldsymbol{\tau} + f\|^2. \tag{3.2}$$

Here $\boldsymbol{\tau} \in H(\Omega, \mathrm{div})$ is a "free" vector-valued function and $C_{\Omega,\underline{A}}$ is a constant in the following Friedrich's type inequality

$$\|v\| \le C_{\Omega,\underline{A}} \|\nabla v\|_a, \quad \forall v \in \mathcal{V}_0. \tag{3.3}$$

If $\Omega \subset \Omega_\square$, then $C_{\Omega,\underline{A}} \le c_2 \frac{l}{\sqrt{d}\pi}$, where $\Omega_\square$ is a square domain with the side l, the constant c_2 comes from (2.2), and d denotes the dimension of the problem. We denote the right hand side of (3.1), which is the upper bound of the true error in the DG approximation u_h, by $M_\oplus^{\mathrm{DG}}$.

Remark 3.1. *The upper bound in (3.1) is sharp since for $\boldsymbol{\tau} = \underline{A}\nabla u$ and $\tilde{u}_h = u$ the right hand side coincides with the left hand one. Thus, the upper bound computed with the help of these functions is as close to the exact error norm as it is desired. Moreover, these estimates do not have any mesh dependence, contain no generic (unknown) constants and do not require Galerkin orthogonality.*

As noted in [35], to obtain sharp estimates for a general problem it is required to minimize the `majorant` $M_\oplus$, a quadratic functional in $\boldsymbol{\tau}$ and β, in (3.2). Since this will involve the solution of a linear system of equations for a vector-valued function $\boldsymbol{\tau} \in H(\Omega, \mathrm{div})$ this process is not cheap. In fact, for difficult problems the cost of sharp estimates can be comparable to (or exceed) the cost of the DG solution. We shall present such an example later in this Section.

3.1. Minimization of the majorant. The majorant (3.2) is a quadratic functional in β and $\boldsymbol{\tau}$. Therefore, we apply an inter-leaved process for its minimization. First, we fix some β and minimize with respect to $\boldsymbol{\tau}$, and then using thus computed $\boldsymbol{\tau}$ we minimize with respect to β.

Minimization with respect to $\boldsymbol{\tau}$: Assuming β is given, let us denote $(1+\beta)$ by a_1 and $(1+1/\beta)C^2_{\Omega,\underline{A}}$ by a_2. Then

$$M_\oplus(\boldsymbol{\tau}) = a_1 \int_\Omega \underline{A}^{-1} (\underline{A}\nabla\tilde{u}_h - \boldsymbol{\tau})^2 \, dx + a_2 \int_\Omega (\mathrm{div}\,\boldsymbol{\tau} + f)^2 \, dx.$$

Differentiating $M_\oplus(\boldsymbol{\tau})$ with respect to $\boldsymbol{\tau}$ (in the sense of Gâteaux) gives

$$M_\oplus(\boldsymbol{\tau})' = 2a_1 \int_\Omega \underline{A}^{-1} (\underline{A}\nabla\tilde{u}_h - \boldsymbol{\tau}) \cdot (-\tilde{\boldsymbol{\tau}}) \, dx + 2a_2 \int_\Omega (\mathrm{div}\,\boldsymbol{\tau} + f)(\mathrm{div}\,\tilde{\boldsymbol{\tau}}) \, dx,$$

where $\tilde{\boldsymbol{\tau}} \in H(\Omega, \mathrm{div})$ denotes a small variation in $\boldsymbol{\tau}$. Substituting $M_\oplus(\boldsymbol{\tau})' = 0$ for minimization, we get

$$a_1 \int_\Omega \underline{A}^{-1}\boldsymbol{\tau} \cdot \tilde{\boldsymbol{\tau}} \, dx + a_2 \int_\Omega \mathrm{div}\,\boldsymbol{\tau}\, \mathrm{div}\,\tilde{\boldsymbol{\tau}} \, dx = a_1 \int_\Omega \nabla\tilde{u}_h \cdot \tilde{\boldsymbol{\tau}} \, dx - a_2 \int_\Omega f \, \mathrm{div}\,\tilde{\boldsymbol{\tau}} \, dx. \tag{3.4}$$

Since $\tilde{u}_h$ and f are known, the solution of this equation gives $\boldsymbol{\tau}$.

Minimization with respect to β: Assuming $\boldsymbol{\tau}$ is known (from the previous step), let us denote

$$b_1 = \int_\Omega \underline{A}^{-1} (\underline{A}\nabla\tilde{u}_h - \boldsymbol{\tau})^2 \, dx, \quad b_2 = \int_\Omega (\mathrm{div}\,\boldsymbol{\tau} + f)^2 \, dx.$$

Note that, since $\tilde{u}_h$ and f are already known, the computation of b_1 and b_2 needs only the evaluation of these integrals, which does not incur any expensive computational overhead. Then,

$$M_\oplus(\beta) = b_1(1+\beta) + b_2(1+1/\beta)C^2_{\Omega,\underline{A}}.$$

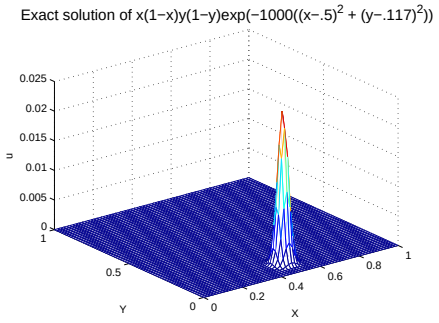

FIG. 3.1. *Illustration of the analytic solution of Example 3.1*

TABLE 3.1
Effectivity and relative computing cost of the majorant for Example 3.1, $p_u = 2$ *(i.e.,* $u_h \in Q_2(K)$*),* $|[\tilde{u}_h - u_h]|^2 = 2.826e-08$

p_τ	β	$\|\underline{A}\nabla\tilde{u}_h - \boldsymbol{\tau}\|^2_{\underline{a}}$	$\|\mathrm{div}\,\boldsymbol{\tau} + f\|^2$	$I_\oplus$	$R^T_{M_\oplus}$
2	3.655	2.524e-03	6.653e-01	15.630	0.914
3	2.047	6.177e-04	5.110e-02	5.070	2.268
4	0.664	3.700e-04	3.217e-03	2.149	4.412
5	0.251	2.310e-04	2.880e-04	1.282	8.214
6	0.047	2.261e-04	9.669e-06	1.062	14.877

Differentiating $M_\oplus(\beta)$ with respect to β gives

$$M_\oplus(\beta)' = b_1 - \frac{b_2 C^2_{\Omega,\underline{A}}}{\beta^2}.$$

Substituting $M_\oplus(\beta)' = 0$ for minimization, we get

$$\beta = \sqrt{\frac{b_2}{b_1}}\, C_{\Omega,\underline{A}}. \tag{3.5}$$

3.2. A motivating example. We now consider a categorically chosen example to show the relative cost of the majorant.

EXAMPLE 3.1. *Consider the Poisson problem on the unit square. Choose* f *and the Dirichlet boundary condition such that the exact (analytic) solution of the problem, which is shown in Figure 3.1, is given by* $u = x(1-x)y(1-y)e^{-1000((x-.5)^2+(y-.117)^2)}$ *[25].* In Table 3.1 we present the effectivity and relative computing cost of the majorant. By p_u and p_τ we denote the polynomial order for the computation of u_h and $\boldsymbol{\tau}$, respectively. The effectivity of the majorant $I_\oplus$ is defined as $I_\oplus = \frac{M^{\mathrm{DG}}_\oplus}{|[u-u_h]|}$. Further, if t_{DG} and $t_{M_\oplus}$ denote the time required for the DG approximation and the majorant $M^{\mathrm{DG}}_\oplus$, respectively, then the relative cost of the majorant can be defined as $R^T_{M_\oplus} = t_{M_\oplus}/t_{\mathrm{DG}}$. These computations are performed using the direct solver of `matlab` on a 4 dual core Intel Xeon MP processors machine with 64 GB RAM. We see that even for this admittedly difficult problem we can get as close to the true error as we please (the effectivity index approaching the academic value one), though with associated high cost. It should be noted, however, that this example is to illustrate the robustness of the majorant technique even for a fixed DG approximation. In practice, it is normally sufficient to take $p_\tau = p_u + 1$ (which corresponds to the right order of the Raviart-Thomas space).

3.3. The discrete problem. The inner product in $H(\Omega, \mathrm{div})$ is given by (see e.g. [5])

$$\Lambda(\boldsymbol{u}, \boldsymbol{v}) = (\boldsymbol{u}, \boldsymbol{v}) + (\mathrm{div}\, \boldsymbol{u}, \mathrm{div}\, \boldsymbol{v}), \quad \forall \boldsymbol{u}, \boldsymbol{v} \in H(\Omega, \mathrm{div}),$$

where $(\cdot, \cdot)$ denotes the inner product in L^2. Therefore, the left hand side of equation (3.4) represents an equivalent inner product in $H(\Omega, \mathrm{div})$. Note that, $M_{\oplus}$, which underlies the derivation of the equation (3.4), is a convex functional and *not* an elliptic boundary value problem. Also, there are *no* associated boundary conditions.

We choose our reference element $\hat{K}$ as $[-1, 1] \times [-1, 1]$. The best known example of shape functions on the reference square for the construction of a finite-dimensional subspace of $H(\Omega, \mathrm{div})$ is the Raviart-Thomas space of index r (denoted by RT_r). It is defined as, for $r \geq 0$,

$$\begin{aligned} \mathrm{RT}_r(\hat{K}) &= (Q_r(\hat{K}))^2 \oplus \boldsymbol{x} Q_r(\hat{K}) = P_{r+1,r}(\hat{K}) \times P_{r,r+1}(\hat{K}) \\ &= \left\{ \boldsymbol{v}(\hat{x}, \hat{y}) : \begin{bmatrix} v^{\hat{x}}(\hat{x}, \hat{y}) \\ v^{\hat{y}}(\hat{x}, \hat{y}) \end{bmatrix} = \begin{bmatrix} \sum_{i=0}^{r+1} \sum_{j=0}^{r} a_{i,j}^{\hat{x}} \hat{x}^i \hat{y}^j \\ \sum_{i=0}^{r} \sum_{j=0}^{r+1} a_{i,j}^{\hat{y}} \hat{x}^i \hat{y}^j \end{bmatrix} \right\}. \end{aligned} \tag{3.6}$$

Thus, the basis for RT_r has the dimension $2(r+1)(r+2)$. Moreover, for $\boldsymbol{v}_r \in \mathrm{RT}_r$ we have

$$\mathrm{div}\, \boldsymbol{v}_r \in Q_r, \quad \boldsymbol{v}_r \cdot \boldsymbol{n}|_{\partial K} \in P_r(\partial K), \quad K \in \mathbb{R}^2, \tag{3.7}$$

where $\boldsymbol{n}$ denotes the outward unit normal vector to the element boundaries. For further details the reader is referred to, e.g., [3, 18]. In this article, as a starting point towards developing the AMLI method for the discretization of $\boldsymbol{\tau} \in H(\Omega, \mathrm{div})$ in (3.4), we restrict ourselves to the lowest order Raviart-Thomas space (RT_0). This will help us to keep the presentation focused and simple, in particular, within the application point of view for a posteriori error estimates. Nevertheless, the development of corresponding AMLI methods for $r \geq 1$ will be the subject of our future work.

Now let $F : \hat{K} \to \mathbb{R}^2$ be a diffeomorphism of the reference element $\hat{K}$ onto a physical element K, i.e. $K = F(\hat{K})$. By $\mathcal{J}$ we denote the Jacobian matrix of the mapping and by $\mathcal{J}_D$ its determinant, which are defined as

$$\mathcal{J} = \begin{pmatrix} x_{\hat{x}} & x_{\hat{y}} \\ y_{\hat{x}} & y_{\hat{y}} \end{pmatrix}, \quad \mathcal{J}_D = |\det \mathcal{J}| = x_{\hat{x}} y_{\hat{y}} - x_{\hat{y}} y_{\hat{x}} > 0.$$

We know that for functions in $H(\Omega, \mathrm{div})$ the Piola transform is a natural choice for the mapping between the reference element $\hat{K}$ and the physical element K, see, e.g. [3, 18]. As a requirement for $H(\Omega, \mathrm{div})$ functions it preserves the normal continuity . It is defined by

$$\boldsymbol{q} = \mathcal{P}_K \hat{\boldsymbol{q}} = \frac{1}{\mathcal{J}_D} \mathcal{J} \hat{\boldsymbol{q}}, \quad \boldsymbol{q} \in H(K, \mathrm{div}), \hat{\boldsymbol{q}} \in H(\hat{K}, \mathrm{div}). \tag{3.8}$$

The Piola transform has the following useful properties

$$\begin{aligned} &\mathrm{div}\, \boldsymbol{q} = \frac{1}{\mathcal{J}_D} \mathrm{div}\, \hat{\boldsymbol{q}}, \quad \nabla p = \mathcal{J}^{-t} \nabla \hat{p}, \\ &\int_K \boldsymbol{q} \cdot \nabla p \, dK = \int_{\hat{K}} \hat{\boldsymbol{q}} \cdot \nabla \hat{p} \, d\hat{K}, \quad \int_K p \, \mathrm{div}\, \boldsymbol{q} \, dK = \int_{\hat{K}} \hat{p} \, \mathrm{div}\, \hat{\boldsymbol{q}} \, d\hat{K}, \\ &\int_{\partial K} p \boldsymbol{q} \cdot \boldsymbol{n} \, dK = \int_{\partial \hat{K}} \hat{p} \hat{\boldsymbol{q}} \cdot \hat{\boldsymbol{n}} \, d\hat{K}, \end{aligned} \tag{3.9}$$

where $p = F(\hat{p})$, $\boldsymbol{q} = \mathcal{P}_K \hat{\boldsymbol{q}}$, and $\boldsymbol{n}$ and $\hat{\boldsymbol{n}}$ denote the unit outward normal vectors on ∂K and $\partial \hat{K}$, respectively.

Now let us denote the element matrices for $\int_K \underline{A}^{-1}\boldsymbol{\tau}\cdot\tilde{\boldsymbol{\tau}}\,dx$ by D_K, and for $\int_K \operatorname{div}\boldsymbol{\tau}\operatorname{div}\tilde{\boldsymbol{\tau}}\,dx$ by C_K. If $\underline{A} = I$ then for the RT_0 elements on the reference square they have the following structure

$$D_K = \begin{bmatrix} 1/3 & 1/6 & 0 & 0 \\ 1/6 & 1/3 & 0 & 0 \\ 0 & 0 & 1/3 & 1/6 \\ 0 & 0 & 1/6 & 1/3 \end{bmatrix}, \quad C_K = \frac{1}{h^2}\begin{bmatrix} 1 & -1 & 1 & -1 \\ -1 & 1 & -1 & 1 \\ 1 & -1 & 1 & -1 \\ -1 & 1 & -1 & 1 \end{bmatrix}. \tag{3.10}$$

The overall element matrix can then be written as

$$A_K = a_1 D_K + a_2 C_K. \tag{3.11}$$

Note that, for fixed $C_{\Omega,\underline{A}}$ and β (which is also small), the C_K part dominates the element matrices as $h \to 0$. Thus, the near nullspace of the element matrix A_K is given by the nullspace of the matrix C_K, which is associated with the local bilinear form

$$C_K(\boldsymbol{u},\boldsymbol{v}) := (\operatorname{div}\boldsymbol{u},\operatorname{div}\boldsymbol{v})_K = \int_K \operatorname{div}\boldsymbol{u}\operatorname{div}\boldsymbol{v}\,dK. \tag{3.12}$$

Lemma 3.1. (Near nullspace of element matrices). *The element matrices A_K associated with the variational equation (3.4) are symmetric positive definite (SPD). Moreover, the nullspace of the matrix C_K associated with the local bilinear form (3.12) for a general element K with nodal coordinates (x_i, y_i), $i \in \{1,2,3,4\}$, see left picture in Figure 4.1, is given by*

$$\ker(C_K) = \operatorname{span}\{(1,1,0,0)^T, (0,0,1,1)^T, (x_1,x_2,-y_3,-y_4)^T\}. \tag{3.13}$$

Proof. Since the coefficients a_1 and a_2 in (3.11) are positive it follows from equation (3.4) that A_K is SPD for a general element K. Moreover, it can easily be seen that there exist positive constants c_1 and c_2 such that the following inequalities hold:

$$c_1\,\zeta(\boldsymbol{w},\boldsymbol{w}) \le \mathbf{w}^T C_K \mathbf{w} \le c_2\,\zeta(\boldsymbol{w},\boldsymbol{w}). \tag{3.14}$$

Here $\boldsymbol{w}$ is a function that is linear in one component and constant in the other component. The function $\zeta(\cdot,\cdot)$ in (3.14) is defined by

$$\zeta(\boldsymbol{w},\boldsymbol{w}) := \int_K \left(\frac{\partial w_1}{\partial x} + \frac{\partial w_2}{\partial y}\right)^2 dK.$$

Thus (for the particular choice of $\boldsymbol{w}$) we get $C_K\mathbf{w} = 0$ if and only if

$$\boldsymbol{w} = (e + dx,\, f - dy)^T$$

for any constants d, e, and f. By setting either d, e, or f to 1 and the other constants to 0, we obtain the three linear independent vectors $(x_1,x_2,-y_3,-y_4)^T$, $(1,1,0,0)^T$, and $(0,0,1,1)^T$ that span the kernel of C_K, respectively. ∎

Remark 3.2. *When using the lowest order Raviart-Thomas elements the matrices C_K are always of rank one. In the global assembly this yields a matrix $C = \sum_K C_K$, where summation is understood in the sense of assembling, whose rank equals the number of elements in the*

mesh. That is, the kernel of the global matrix C has dimension $\dim(\ker(C)) = n_E - n_K$ *where* n_E *denotes the number of faces and* n_K *the number of elements in the finite element mesh.*[*]

REMARK 3.3. *In case of a uniform mesh composed of square* RT_0 *elements the matrix* C_K *is the same for each element K; Its nullspace then is given by*

$$\ker(C_K) = \mathrm{span}\{(1,1,0,0)^T, (0,0,1,1)^T, (-1,1,1,-1)^T\}.$$

Since the vector $(1,-1,1,-1)^T$ *is orthogonal to the kernel of* C_K *in this case it is clear that the rank-one matrix* C_K *is of the form* $c \cdot (1,-1,1,-1)^T \cdot (1,-1,1,-1)$.

4. Algebraic multilevel iteration. In order to solve the linear system arising from IP-DG approximation (2.5) of the elliptic model problem, based on bilinear elements, we use the AMLI method proposed in Reference [33]. For the solution of the linear system arising from the minimization of the majorant for the a posteriori error estimate, i.e, equation (3.4), we describe and analyze the AMLI method in the remainder of this section.

4.1. The AMLI procedure. The straightforward recursive extension of two-level methods leads to the class of hierarchical basis (HB) methods for which the condition number in general grows exponentially with the number of levels ℓ. Therefore, in order to obtain optimal order solution algorithms, HB preconditioners are combined with various types of stabilization techniques. One particular purely algebraic stabilization technique is the AMLI method, where a specially constructed matrix polynomial P_{β_k} of degree β_k is employed on some (all) levels $k = k_0 + 1, \cdots, \ell$. The AMLI methods have originally been introduced and studied in a multiplicative form, see [8, 9].

Let $\hat{A}^{(k)}$ denote a hierarchical basis (HB) matrix corresponding to a k times refined mesh $\mathcal{T}_{h_k}$ where $0 \le k \le \ell$. Details on the HB transformation will follow in the next subsection. Further let $M^{(k)}$ denote a preconditioner for $\hat{A}^{(k)}$; The task is then to construct the preconditioner $M^{(\ell)}$ for the HB matrix $\hat{A}^{(\ell)} := \hat{A}_h$. For convenience, let $\hat{A}^{(k)}_{ij}$ denote the blocks of the two-level HB matrix $\hat{A}^{(k)}$ at level k.

Starting at level 0 (associated with the coarsest mesh) on which a complete LU factorization of the matrix $\hat{A}^{(0)}$ is performed, we define

$$M^{(0)} := \hat{A}^{(0)}. \tag{4.1}$$

After k steps of (regular) mesh refinement the multiplicative preconditioner $M^{(k)}$ at level k can be defined via its inverse

$$M^{(k)^{-1}} := U^{(k)} D^{(k)} L^{(k)} \tag{4.2}$$

where

$$U^{(k)} := \begin{pmatrix} I & -C_{11}^{(k)^{-1}} \hat{A}_{12}^{(k)} \\ 0 & I \end{pmatrix}, \quad L^{(k)} := \begin{pmatrix} I & 0 \\ -\hat{A}_{21}^{(k)} C_{11}^{(k)^{-1}} & I \end{pmatrix} \tag{4.3}$$

and

$$D^{(k)} := \begin{pmatrix} C_{11}^{(k)^{-1}} & 0 \\ 0 & C_{22}^{(k)^{-1}} \end{pmatrix}. \tag{4.4}$$

Here $C_{11}^{(k)}$ is a preconditioner for the upper-left pivot block $\hat{A}_{11}^{(k)}$ of the HB matrix

$$\hat{A}^{(k)} = \begin{bmatrix} \hat{A}_{11}^{(k)} & \hat{A}_{12}^{(k)} \\ \hat{A}_{21}^{(k)} & \hat{A}_{22}^{(k)} \end{bmatrix},$$

[*]Thus the dimension of the kernel is usually of the same order as the total number of DOF.

and the matrix $C_{22}^{(k)}$ is implicitly given by the equation

$$C_{22}^{(k)^{-1}} = \left[I - P_\beta(M^{(k-1)^{-1}}\hat{A}^{(k-1)})\right](\hat{A}^{(k-1)})^{-1} \tag{4.5}$$

with $M^{(k-1)}$ and $\hat{A}^{(k-1)}$ denoting the preconditioner and the HB matrix at level $(k-1)$, respectively.[†] Then, as is well known from theory [8, 9], a properly shifted and scaled Chebyshev polynomial P_β of degree β, satisfying the conditions

$$0 \le P_\beta(t) < 1, \quad 0 < t \le 1, \quad P_\beta(0) = 1,$$

can be used to stabilize the condition number of $M^{(\ell)^{-1}}\hat{A}^{(\ell)}$. From the latter condition on P_β one finds that (4.5) is equivalent to

$$C_{22}^{(k)^{-1}} = M^{(k-1)^{-1}}Q^{(k)}(\hat{A}^{(k-1)}M^{(k-1)^{-1}}). \tag{4.6}$$

where the polynomial $Q^{(k)}$ is given by

$$Q^{(k)}(t) = \frac{1 - P_\beta^{(k)}(t)}{t}. \tag{4.7}$$

Alternatively, in the nonlinear AMLI method, a few inner generalized conjugate gradient (GCG) type iterations are performed in order to improve (or freeze) the convergence factor of the outer GCG iteration. Under certain conditions, see e.g., [31], this results in a constant (mesh-independent) number of outer iterations (uniformly bounded in the number of levels). The whole iterative solution process is of optimal order of computational complexity if the degree $\beta_k = \beta$ of the matrix polynomial (or alternatively, the number of inner iterations for nonlinear AMLI) at level k satisfies the optimality conditions

$$1/\sqrt{(1-\gamma^2)} < \beta < \tau, \tag{4.8}$$

where $\tau \approx \tau_k = N_k/N_{k-1}$ denotes the reduction factor of the number of DOF, and γ denotes the constant in the strengthened Cauchy-Bunyakowski-Schwarz (CBS) inequality. The CBS inequality constant, as will be pointed out in Section 4.3, plays an important role in the construction and in the analysis of AMLI methods. The value of τ is exactly 4 for DG approximations of 2D problems and it is approximately 4 in our RT_0 finite element computation of the corresponding majorant (3.4).

4.2. Hierarchical splitting of the lowest order Raviart-Thomas space. The AMLI methods we are considering here for the minimization of the majorant (3.2) are based on a proper splitting of the RT_0 subspace of $H(\Omega, \mathrm{div})$. The particular two-level HB transformation that induces this splitting was introduced earlier in the context of Rannacher-Turek type elements [24]. It is briefly described for the lowest order Raviart-Thomas space in the following.

Consider two consecutive discretizations $\mathcal{T}_H$ and $\mathcal{T}_h$. Figure 4.1 illustrates a macro-element G obtained after one regular mesh-refinement step. We see that in this case the corresponding finite element spaces $\mathcal{V}_H$ and $\mathcal{V}_h$ are not nested. Let $\varphi_G = \{\phi_i(x,y)\}_{i=1}^{12}$ be the macro-element vector of the nodal basis functions and A_G be the macro-element stiffness matrix corresponding to $G \in \mathcal{T} = \mathcal{T}_h$. The global stiffness matrix A_h can be written as

$$A_h = \sum_{G\in\mathcal{T}} A_G$$

[†]On the coarsest level (with index 0) we have $\hat{A}^{(0)} = A^{(0)}$, i.e., no HB transformation is applied there.

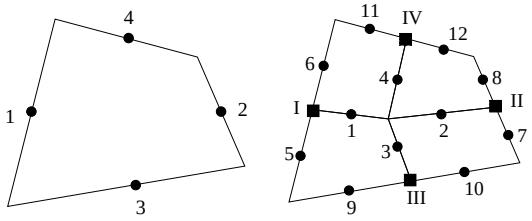

FIG. 4.1. *Macro-element obtained after one regular mesh-refinement step*

where the summation is understood in the sense of assembling the (12×12) matrices A_G. Using the local numbering of DOF as shown in Figure 4.1 (right picture) a macro-element level transformation matrix J_G is constructed based on differences and aggregates of those basis functions ϕ_i that correspond to nodes that are shared by adjacent macro elements, i.e.,

$$J_G^T = \frac{1}{2}\begin{bmatrix} 2 & & & & & & & & & & & \\ & 2 & & & & & & & & & & \\ & & 2 & & & & & & & & & \\ & & & 2 & & & & & & & & \\ & & & & 1 & -1 & & & & & & \\ & & & & & & 1 & -1 & & & & \\ & & & & & & & & 1 & -1 & & \\ & & & & & & & & & & 1 & -1 \\ & & & & 1 & 1 & & & & & & \\ & & & & & & 1 & 1 & & & & \\ & & & & & & & & 1 & 1 & & \\ & & & & & & & & & & 1 & 1 \end{bmatrix}, \tag{4.9}$$

see [24]. This transformation defines locally a two-level hierarchical basis $\hat{\varphi}_G$, namely, $\hat{\varphi}_G = J_G^T \varphi_G$. Then the hierarchical two-level macro-element matrix is given by

$$\hat{A}_G = J_G^T A_G J_G,$$

and the related global two-level matrix can be obtained via assembling, i.e.,

$$\hat{A}_h = \sum_{G \in \mathcal{T}} \hat{A}_G,$$

or, alternatively, via the transformation

$$\hat{A}_h = J^T A_h J,$$

where the global transformation matrix J is induced by the J_G's, i.e.,

$$J_G = J|_G \quad \forall G \in \mathcal{T}.$$

We partition now the two-level stiffness matrix $\hat{A}_h$ into 2×2 blocks, i.e.,

$$\hat{A}_h = \begin{bmatrix} \hat{A}_{11} & \hat{A}_{12} \\ \hat{A}_{21} & \hat{A}_{22} \end{bmatrix}, \tag{4.10}$$

where $\hat{A}_{11}$ corresponds to the interior unknowns with respect to the macro-elements $G \in \mathcal{T}$. The idea of the "first reduce" (FR) approach is to eliminate these unknowns. This static condensation step can be written in the form

$$\hat{A}_h = \begin{bmatrix} \hat{A}_{11} & 0 \\ \hat{A}_{21} & B \end{bmatrix} \begin{bmatrix} I_1 & \hat{A}_{11}^{-1}\hat{A}_{12} \\ 0 & I_2 \end{bmatrix}, \tag{4.11}$$

with the (exact) Schur complement $B = \hat{A}_{22} - \hat{A}_{21}\hat{A}_{11}^{-1}\hat{A}_{12}$. Next the matrix B is partitioned into 2×2 blocks, i.e.,

$$B = \begin{bmatrix} B_{11} & B_{12} \\ B_{21} & B_{22} \end{bmatrix}, \tag{4.12}$$

where the first block corresponds to the difference basis functions and the second to the aggregates, which are associated with the coarse grid. This algorithm can be applied recursively on each level $k = \ell, \ell-1, \ldots, 1$.

4.3. Local analysis. In the hierarchical bases context we denote by $\mathcal{V}_1$ and $\mathcal{V}_2$ subspaces of the finite element space $\mathcal{V}_h$. The space $\mathcal{V}_2$ is spanned by the coarse-space basis functions (aggregates) and $\mathcal{V}_1$ is the complement of $\mathcal{V}_2$ in $\mathcal{V}_h$, i.e., $\mathcal{V}_h$ is a direct sum of $\mathcal{V}_1$ and $\mathcal{V}_2$:

$$\mathcal{V}_h = \mathcal{V}_1 \oplus \mathcal{V}_2 \tag{4.13}$$

A measure for the quality of this splitting is the constant γ in the strengthened CBS inequality, which is defined by

$$\gamma = \cos(\mathcal{V}_1, \mathcal{V}_2) := \sup_{\boldsymbol{u} \in \mathcal{V}_1,\ \boldsymbol{v} \in \mathcal{V}_2} \frac{\mathcal{A}(\boldsymbol{u}, \boldsymbol{v})}{\sqrt{\mathcal{A}(\boldsymbol{u}, \boldsymbol{u})\mathcal{A}(\boldsymbol{v}, \boldsymbol{v})}}.$$

In our case $\mathcal{A}(\cdot,\cdot)$ is the bilinear form that appears in the left-hand side of (3.4), i.e.,

$$\mathcal{A}(\boldsymbol{u}, \boldsymbol{v}) := a_1 \int_\Omega A^{-1}\boldsymbol{u} \cdot \boldsymbol{v}\, d\Omega + a_2 \int_\Omega \operatorname{div} \boldsymbol{u} \operatorname{div} \boldsymbol{v}\, d\Omega. \tag{4.14}$$

It is well known (see e.g. [7]) that γ can be estimated locally, in our case over each macro element G, which means that $\gamma = \max_G \gamma_G$, where

$$\gamma_G := \sup_{\boldsymbol{u} \in \mathcal{V}_1(G),\ \boldsymbol{v} \in \mathcal{V}_2(G)} \frac{\mathcal{A}_G(\boldsymbol{u}, \boldsymbol{v})}{\sqrt{\mathcal{A}_G(\boldsymbol{u}, \boldsymbol{u})\mathcal{A}_G(\boldsymbol{v}, \boldsymbol{v})}}.$$

The spaces $\mathcal{V}_k(G)$ above contain the functions from $\mathcal{V}_k$ restricted to G and $\mathcal{A}_G(\boldsymbol{u}, \boldsymbol{v})$ corresponds to $\mathcal{A}(\boldsymbol{u}, \boldsymbol{v})$ restricted over the macro element G.

We perform this local analysis on the matrix level, where the splitting (4.13) is obtained via the two-level hierarchical basis transformation described earlier, and the space $\mathcal{V}_h$ corresponds to the choice of lowest order Raviart-Thomas elements. In this setting the upper left block of $\hat{A}_h$ is block-diagonal (with diagonal blocks of $\hat{A}_{11}$ of size 4×4 which can be associated with the interior nodes $\{1, 2, 3, 4\}$ in the right picture of Figure 4.1). Therefore, we first compute the local Schur complements arising from static condensation of the interior DOF and obtain hereby the (8×8) matrices B_G. Next we split each matrix B_G as

$$B_G = \begin{bmatrix} B_{G,11} & B_{G,12} \\ B_{G,21} & B_{G,22} \end{bmatrix} \begin{matrix} \} \text{ differences} \\ \} \text{ aggregates} \end{matrix}$$

written again in two-by-two block form (with blocks of size 4×4). We have thus reduced the problem of estimating the CBS constant of the splitting (4.13) to a small-sized local problem that involves the matrix B_G. Following the general theory, see [7, 21], it suffices to compute the minimal eigenvalue of the generalized eigenproblem

$$S_G\mathbf{v}_G = \lambda_{G,\min} B_{G,22}\mathbf{v}_G, \quad \forall \mathbf{v}_G, \tag{4.15}$$

where $S_G = B_{G,22} - B_{G,21}B_{G,11}^{-1}B_{G,12}$, and then

$$\gamma^2 \le \max_{G\in\mathcal{T}} \gamma_G^2 = \max_{G\in\mathcal{T}}(1-\lambda_{G,\min}). \tag{4.16}$$

The following theorem provides a theoretical estimate that holds on all levels of recursive splitting of the RT_0 subspace of $H(\Omega,\mathrm{div})$.

THEOREM 4.1. *Consider the approximation of the equation (3.4), posed in $H(\Omega,\mathrm{div})$, using the RT_0 subspace associated with an equidistant two-dimensional rectangular mesh. Under these assumptions the CBS constant γ related to the hierarchical splitting (4.13) has the upper bound $\gamma \le \gamma_G < \sqrt{3/8}$. Moreover, this bound holds also in each step of a recursive hierarchical splitting.*

Proof. In order to prove this uniform bound for γ we study the generalized eigenproblem (4.15). At level ℓ of the finest discretization the macro-element matrix $\hat{A}_G$, which is the same for all G in $\mathcal{T}_{h_\ell}$ for a uniform mesh, can be represented in the form

$$\hat{A}_G^{(0)} = J_G^T\left(\sum_{K\in G\subset\mathcal{T}_{h_\ell}} A_K^{(0)}\right)J_G = d_0 J_G^T\left(\sum_{K\in G\subset\mathcal{T}_{h_\ell}} D_K^{(0)} + \sum_{K\in G\subset\mathcal{T}_{h_\ell}} \bar{C}_K\right)J_G \tag{4.17}$$

where

$$D_K^{(0)} = \begin{bmatrix} e_0 & f_0 & 0 & 0\\ f_0 & e_0 & 0 & 0\\ 0 & 0 & e_0 & f_0\\ 0 & 0 & f_0 & e_0 \end{bmatrix}, \qquad \bar{C}_K = \begin{bmatrix} 1 & -1 & 1 & -1\\ -1 & 1 & -1 & 1\\ 1 & -1 & 1 & -1\\ -1 & 1 & -1 & 1 \end{bmatrix} \quad \forall K\in G\ \forall G\subset\mathcal{T}_{h_\ell},$$

and the local transformation matrix J_G is defined according to (4.9). The positive constants d_0, e_0, and f_0 clearly depend on a_1 and a_2, cf. (3.4), as well as on the mesh size h, see (3.10). However, we have $e_0 = 2f_0$.

Dividing (4.17) by d_0, which does not change the (estimate of the) local CBS constant γ_G, the Schur complement S_G and the lower-right 4×4 block of the matrix B_G for the first splitting (at level ℓ) are to be found

$$S_G^{(0)} = \begin{bmatrix} s_0 & t_0 & 1/4 & -1/4\\ t_0 & s_0 & -1/4 & 1/4\\ 1/4 & -1/4 & s_0 & t_0\\ -1/4 & 1/4 & t_0 & s_0 \end{bmatrix}$$

and

$$B_{G,22}^{(0)} = \begin{bmatrix} p_0 & q_0 & 1/4 & -1/4\\ q_0 & p_0 & -1/4 & 1/4\\ 1/4 & -1/4 & p_0 & q_0\\ -1/4 & 1/4 & q_0 & p_0 \end{bmatrix}$$

with

$$
\begin{aligned}
s_0 &= \frac{2e_0(1+e_0(3+e_0))+2e_0f_0-(1+e_0)f_0^2}{4e_0(2+e_0)},\\
t_0 &= -\frac{f_0^2+e_0(2+(-2+f_0)f_0)}{4e_0(2+e_0)},\\
p_0 &= \frac{1+2e_0(2+e_0)-(-2+f_0)f_0}{4(1+e_0)},\\
q_0 &= -\frac{(-1+f_0)^2}{4(1+e_0)},
\end{aligned}
$$

respectively. The generalized eigenproblem (4.15) has two different two-fold eigenvalues, namely $\lambda_{1,2}=1$ and

$$\lambda_{3,4}=\frac{(1+e_0)(e_0(3+e_0)-(1+e_0)f_0)}{e_0(2+e_0)(2+e_0-f_0)}$$

which shows that

$$\left(\gamma_G^{(0)}\right)^2 \le 1-\lambda_{3,4}=\frac{e_0+f_0}{e_0(2+e_0)(2+e_0-f_0)}. \tag{4.18}$$

In order to compute a similar bound for the second splitting (at level $\ell-1$) we have to use the relation $A_K^{(1)} := B_{G,22}^{(0)}$. In general, for the $(k+1)$-th splitting (at level $\ell-k$) the relation

$$A_K^{(k)} := B_{G,22}^{(k-1)} \tag{4.19}$$

is to be used in the assembly of A_G, i.e.,

$$\hat{A}_G^{(k)} = J_G^T\left(\sum_{K\in G\subset\mathcal{T}_{h_{\ell-k}}} A_K^{(k)}\right)J_G. \tag{4.20}$$

Repeating the computations once, we find that the representation

$$\hat{A}_G^{(k)} = d_k J_G^T\left(\sum_{K\in G\subset\mathcal{T}_{h_{\ell-k}}} D_K^{(k)} + \sum_{K\in G\subset\mathcal{T}_{h_{\ell-k}}} \bar{C}_K\right)J_G \tag{4.21}$$

holds for all $k=1,2,\ldots$ with some positive constants d_k where we have retained unchanged the matrix $\bar{C}_K$. The matrices

$$D_K^{(k)} = \begin{bmatrix} e_k & f_k & 0 & 0\\ f_k & e_k & 0 & 0\\ 0 & 0 & e_k & f_k\\ 0 & 0 & f_k & e_k \end{bmatrix}$$

can be computed via the recurrence relations

$$e_k = \frac{3e_{k-1}+2(e_{k-1})^2+2f_{k-1}-(f_{k-1})^2}{1+e_{k-1}}, \tag{4.22a}$$

$$f_k = \frac{e_{k-1}+2f_{k-1}-(f_{k-1})^2}{1+e_{k-1}}. \tag{4.22b}$$

Thus the bound for γ_G at level $\ell - k$ reads

$$\left(\gamma_G^{(k)}\right)^2 \le \frac{e_k + f_k}{e_k(2+e_k)(2+e_k-f_k)} =: g(e_k, f_k) \tag{4.23}$$

with e_k and f_k given by (4.22). Further $e_0 = \frac{1}{3}\frac{a_1}{a_2}h^2 = \frac{1}{3}\frac{\beta}{C^2_{\Omega,A}}h^2$, and $f_0 = \frac{1}{2}e_0$. Using $0 < f_{k-1} \le \frac{1}{2}e_{k-1}$ it follows by induction that $f_k > 0$ and that

$$\frac{f_k}{e_k} \le \frac{4 - f_{k-1}}{8 + 7f_{k-1}} < \frac{1}{2}$$

for all k. Finally we have

$$g(e_k, f_k) = \frac{e_k + f_k}{e_k(2+e_k)(2+e_k-f_k)} \le \frac{\frac{3}{2}e_k}{e_k(2+e_k)(2+\frac{1}{2}e_k)} = \frac{\frac{3}{2}}{4 + 3e_k + \frac{1}{2}e_k^2} < \frac{3}{8},$$

which completes the proof. □

REMARK 4.1. *The upper bound* $3/8$ *for* γ_G^2*, and thus for* γ*, is quite pessimistic on (very) coarse levels as can be seen by Figure 4.2. The curves from left to right show the behavior of* $g(e_k, f_k)$ *as defined by (4.23) using the relations (4.22) for decreasing values of the parameter* β*. We observe that* γ_G^2 *approaches zero when the splitting is applied many times, which means that the two subspaces* $\mathcal{V}_1$ *and* $\mathcal{V}_2$ *in (4.13) become more and more orthogonal to each other as the recursion proceeds.*

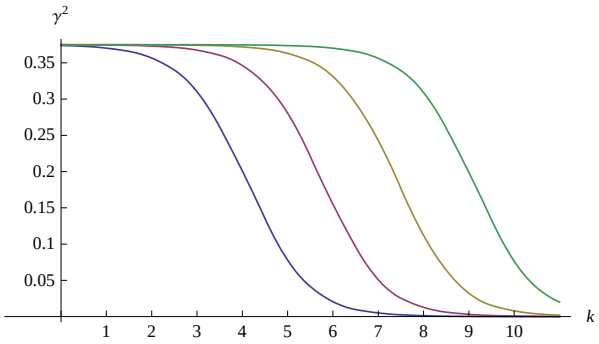

FIG. 4.2. *Multilevel behavior of* γ_G^2 *for unit square:* $h = 1/128$*;* $\beta = 10, 1, 0.1, 0.01$ *(left to right curve)*

REMARK 4.2. *The quantitative bounds on the CBS constant are required in the construction of the matrix polynomials* $Q^{(k)}(t)$*, see (4.7), that are used in the linear AMLI algorithm for stabilizing the condition number. In accordance with the analysis in [8, 9] we use the coefficients*

$$q_0 = \frac{2}{\sqrt{1-\gamma^2}}, \quad q_1 = -\frac{1}{1-\gamma^2} \tag{4.24}$$

in the polynomial $Q^{(k)}(t) = Q_W(t) = q_0 + q_1 t$ *for the linear AMLI W-cycle (at all intermediate levels* $k = \ell - 1, \ell - 2, \ldots, 1$*) where we insert the upper bound* $3/8$ *for* γ*. Though this choice is theoretically founded for the case of exact inversion of the pivot block* $\hat{A}_{11}$ *only, the numerical results presented in the next section suggest that it works also when using an approximate inversion of* $\hat{A}_{11}$*.*

TABLE 5.1
Effectivity of the majorant for Example 5.1

$1/h$	β	$\|[\![\tilde{u}_h - u_h]\!]\|$	$\|\underline{A}\nabla\tilde{u}_h - \boldsymbol{\tau}\|_a^2$	$\|\mathrm{div}\,\boldsymbol{\tau} + f\|^2$	$I_\oplus$
32	2.5e-05	5.940e-07	4.089e-05	5.202e-13	1.122
64	3.0e-06	7.796e-08	1.020e-05	2.010e-15	1.088
128	0.0e-06	1.037e-08	2.546e-06	7.792e-18	1.064
256	0.0e-06	1.434e-09	6.362e-07	3.030e-20	1.047
512	0.0e-06	2.125e-10	1.590e-07	1.182e-22	1.036
1024	0.0e-06	3.481e-11	3.974e-08	1.156e-23	1.029
2048	0.0e-06	6.408e-12	9.935e-09	1.985e-25	1.025

5. Numerical results. For the approximation of the vector-valued function $\boldsymbol{\tau}$ and the DG approximation u_h we use the spaces RT_0, and $Q_1(K)$, respectively. The domain is discretized by a rectangular mesh and the coarsest mesh in all computations is of size 16×16. The finer meshes are of the sizes $1/h = 32, 64, 128, 256, 512, 1024, 2048$ (i.e. upto 8 392 704 DOF). The $\hat{A}_{11}$ block is approximated by using an incomplete LU factorization without (additional) fill-in [46]. In the nonlinear AMLI method we have employed a fixed small number ν ($\nu = 2$ corresponding to the classical W-cycle) of inner generalized conjugate gradient (GCG) iterations at every coarse level except the coarsest one where we use a direct solve (complete LU factorization). The starting vector for the outer iteration is the zero vector and the stopping criteria is

$$\|r^{(n_{\mathrm{it}})}\|/\|r^{(0)}\| \le \delta = 10^{-6},$$

where n_{it} is the number of iterations we report in the tables. The average residual reduction factor ρ is defined as

$$\rho := \left(\|r^{(n_{\mathrm{it}})}\|/\|r^{(0)}\|\right)^{\frac{1}{n_{\mathrm{it}}}}.$$

The numerical experiments, which are performed on a Fujitsu Siemens Primergy RX600 S3 workstation with 4 dual core Intel Xeon MP processors (3.4GHz) and 64 GB RAM, comprise the following examples.

EXAMPLE 5.1. *Consider the Poisson problem on the unit square and choose f and the Dirichlet boundary conditions such that the analytic solution of the problem is given by $u = 1/4(x(1-x) + y(1-y))$.*

EXAMPLE 5.2. *Consider the Poisson problem on the unit square with homogenous Dirichlet boundary conditions and choose f such that the analytic solution of the problem is given by $u = \sin 2\pi x \sin 2\pi y$.*

First, we discuss the results related to a posteriori error estimates. In Tables 5.1 and 5.2 we present various components of the majorant (see equations (3.1-3.2)) and the effectivity index of the majorant for Examples 5.1 and 5.2, respectively. Note that, because $\tilde{u}_h$ is taken as an orthogonal projection of u_h, the nonconformity error ($|[\![\tilde{u}_h - u_h]\!]|$) is very small as compared to the other terms of the majorant. Further, the divergence of any function in the RT_0 space is a constant function. Because f is also a constant for Example 5.1 we see that the flux equilibration term (div $\tau + f$) is negligibly small. The majorant is thus represented mainly by the error in the duality relation for fluxes and a sharp upper bound of the error is obtained, with the effectivity index being close to one. The convergence of the true error and the majorant is shown in Figure 5.1(a).

The function f, on the other hand, has steep gradients for Example 5.2. The flux equilibration term, resulting from the approximation of f by a constant function (div τ), is therefore

TABLE 5.2
Effectivity of the majorant for Example 5.2

$1/h$	β	$\|[\tilde{u}_h - u_h]\|$	$\|\|\underline{A}\nabla\tilde{u}_h - \boldsymbol{\tau}\|\|_a^2$	$\|\|\mathrm{div}\,\boldsymbol{\tau} + f\|\|^2$	$I_\oplus$
32	2.0095	6.105e-04	1.254e-01	9.993e-00	4.278
64	2.0024	7.866e-05	3.162e-02	2.502e-00	4.292
128	2.0006	9.955e-06	7.921e-03	6.258e-01	4.285
256	2.0002	1.251e-06	1.981e-03	1.565e-01	4.275
512	2.0000	1.568e-07	4.954e-04	3.912e-02	4.266
1024	2.0000	1.963e-08	1.239e-04	9.780e-03	4.260
2048	2.0000	2.455e-09	3.097e-05	2.445e-03	4.255

large as compared to the other terms of the majorant. This causes a loss in the sharpness of the upper bound of the error. Nevertheless, because both the functions τ and div τ have first order convergence in the L^2 norm for the RT_0 space on a rectangular mesh, see, e.g. [3, 18], the effectivity index stays bounded. The convergence of the true error and the majorant is shown in Figure 5.1(b).

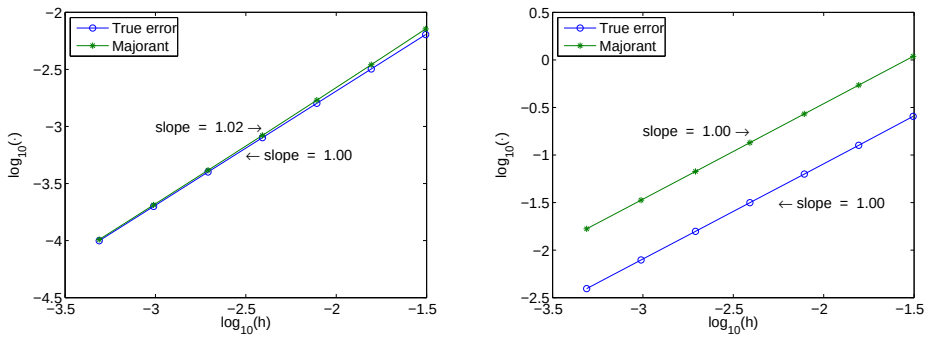

(a) Example 5.1 (b) Example 5.2

FIG. 5.1. *Convergence of the true error and the majorant.*

We now discuss the results on the convergence of the proposed AMLI method. In Tables 5.3, 5.4, and 5.5 we present the number of iterations n_{it} and the average residual reduction factor ρ for the nonlinear AMLI solver with W cycle, the linear AMLI solver with W cycle, and the linear AMLI solver with V cycle, respectively. For the sake of fairness in the comparison of the computing cost we use the AMLI method for the DG discretization of elliptic problems proposed in [33, 34]. By t^S_{DG} and $t^S_{M_\oplus}$ we denote the solution time (including the set-up) required by the AMLI method for the DG problem (2.5) and the problem (3.4), respectively. Further, by $t_r = t^S_{M_\oplus}/t^S_{\mathrm{DG}}$ we denote the relative cost of computing the majorant with respect to the cost of solving the original DG problem.

We observe that t_r is approximately one eighth for both methods, the nonlinear and the linear AMLI W-cycle, see Tables 5.3 and 5.4. In practice, this relative cost is a reasonable overhead for the computation of the *guaranteed and efficient* a posteriori error estimates. Moreover, the optimal computational complexity of the solvers in these cases is reflected by a uniformly bounded (constant) number of outer iterations. The slightly superlinear increase of the solution time against the problem size (number of DOF) may be attributed to our particular implementation.

In case of the linear AMLI V-cycle, see Table 5.5, we find that the relative cost is even

TABLE 5.3
Convergence results and the associated cost of the nonlinear AMLI solver with W cycle

	DG			$H(\Omega, \mathrm{div})$		
$1/h$	n_{it}	ρ	t^S_{DG}	n_{it}	ρ	$t^S_{M_\oplus}$
32	18	0.46	0.08	5	0.05	0.01
64	18	0.46	0.39	6	0.07	0.04
128	18	0.44	1.82	5	0.06	0.16
256	16	0.42	7.55	4	0.03	0.65
512	16	0.41	34.43	4	0.03	3.05
1024	16	0.41	142.17	4	0.02	14.53
2048	16	0.41	574.45	4	0.02	67.58

TABLE 5.4
Convergence results and the associated cost of the linear AMLI solver with W cycle

	DG			$H(\Omega, \mathrm{div})$		
$1/h$	n_{it}	ρ	t^S_{DG}	n_{it}	ρ	$t^S_{M_\oplus}$
32	18	0.45	0.09	5	0.05	0.01
64	19	0.47	0.37	6	0.07	0.03
128	18	0.46	1.71	6	0.09	0.15
256	19	0.47	7.57	7	0.10	0.77
512	19	0.47	32.73	7	0.10	3.62
1024	19	0.48	137.76	7	0.10	17.70
2048	19	0.48	557.75	7	0.10	79.64

smaller. As it is predicted by the classical theory of AMLI methods, the V-cycle, when applied to the linear system arising from the DG problem (2.5), results in an increase of the number of iterations by some (almost) constant factor for each additionally introduced level. This factor can be estimated by $1/\sqrt{1-\gamma^2}$, which is in accordance with the findings in [33] where it was shown that $\gamma^2 \leq 1/2$, cf. Theorem 6.5 in [33]. Indeed, the number of iterations grows by a factor of 1.3 to 1.4 for each newly added level of mesh refinement, see second column of Table 5.5. On the other hand, with the AMLI solver proposed in Section (4) for the problem (3.4) the increase in the number of PCG iterations with V-cycle preconditioning is much slower (even sublinear) against the number of levels, see fifth column of Table 5.5. This is, however, expected from the theoretical bound (4.23) for γ^2, see Figure 4.2, whose improvement from level to level explains the better performance of the AMLI V-cycle on the $H(\mathrm{div})$-conforming discretization of the problem (3.4) as compared to the original DG problem (2.5).

6. Conclusion. We have presented an optimal order AMLI method for problems in the space $H(\Omega, \mathrm{div})$ and their application to the minimization process of functional a posteriori error estimates. The main result of our local analysis (Theorem 4.1) shows that a second order stabilization polynomial, i.e. a $W-$cycle, is sufficient to stabilize the AMLI process, which in the present setting would require a bound $\gamma < \sqrt{3/4}$ at all levels (indeed we obtained $\gamma < \sqrt{3/8}$). Moreover, we derived explicit bounds for the multilevel behavior of γ that demonstrate that even the $V-$cycle variant of AMLI (without stabilization) becomes an almost optimal order solution process. Thereby, we ensure that the sharp bounds of the error are obtained with reasonable cost overhead.

Acknowledgements. The support from the Austrian Academy of Sciences for this research work is gratefully acknowledged. The authors would also like to thank Professor S. Repin for his helpful suggestions on a posteriori error estimates.

TABLE 5.5
Convergence results and the associated cost of the linear AMLI solver with V cycle

	DG			$H(\Omega, \mathrm{div})$		
$1/h$	n_{it}	ρ	t^S_{DG}	n_{it}	ρ	$t^S_{M_\oplus}$
32	18	0.45	0.09	5	0.05	0.01
64	20	0.49	0.34	7	0.12	0.04
128	26	0.59	1.79	8	0.17	0.15
256	36	0.68	8.81	9	0.21	0.80
512	48	0.75	44.56	11	0.28	4.01
1024	65	0.81	227.30	13	0.27	21.82
2048	90	0.86	1173.15	13	0.33	95.13

REFERENCES

[1] Ainsworth M. A posteriori error estimation for discontinuous Galerkin finite element approximation. *SIAM J. Numer. Anal.* 2007; **45**(4): 1777–1798.

[2] Ainsworth M, Oden JT. *A posteriori error estimation in finite element analysis.* Wiley-Interscience, John Wiley & Sons, New York, 2000.

[3] Arnold DN, Boffi D, Falk RS. Quadrilateral $H(\mathrm{div})$ finite elements. *SIAM J. Numer. Anal.*, 2005; **42**:2429–2451.

[4] Arnold DN, Brezzi F, Cockburn B, Marini LD. Unified analysis of discontinuous Galerkin methods for elliptic problems. *SIAM J. Numer. Anal.*, 2002; **39**:1749–1779.

[5] Arnold DN, Falk RS, Winther R. Preconditioning in $H(\mathrm{div})$ and applications. *Math. Comp.*, 1997; **66**:957–984.

[6] Arnold DN, Falk RS, Winther R. Multigrid in $H(\mathrm{div})$ and $H(\mathrm{curl})$. *Numer. Math.*, 2000; **85**:197–217.

[7] Axelsson O, Gustafsson I. Preconditioning and two-level multigrid methods of arbitrary degree of approximations. *Math. Comp.*, 1983; **40**:219–242.

[8] Axelsson O, Vassilevski PS. Algebraic multilevel preconditioning methods I. *Numer. Math.*, 1989; **56**:157–177.

[9] Axelsson O, Vassilevski PS. Algebraic multilevel preconditioning methods II. *SIAM J. Numer. Anal.*, 1990; **27**:1569–1590.

[10] Axelsson O, Vassilevski P. Variable-step multilevel preconditioning methods, I: self-adjoint and positive definite elliptic problems. *Numer. Lin. Alg. Appl.*, 1994; **1**:75–101.

[11] Babuška I, Rheinboldt WC. A posteriori error estimates for the finite element method. *Int. J. Numer. Meth. Engrg.* 1978; **12**: 1597–1615.

[12] Babuška I, Strouboulis T. *The finite element method and its reliability.* Clarendon Press, Oxford University Press, New York, 2001.

[13] Bangerth W, Rannacher R. *Adaptive Finite Element Methods for Differential Equations.* Lectures in Mathematics, ETH Zürich. Birkhäuser, Basel, 2003.

[14] Bank R, Dupont T. An optimal order process for solving finite element equations. *Math. Comp.*, 1981; **36**:427–458.

[15] Becker R, Hansbo P, Larson MG. Energy norm a posteriori error estimation for discontinuous Galerkin methods. *Comput. Methods Appl. Mech. Engrg.* 2003; **192**(5-6): 723–733.

[16] Blaheta R, Margenov S, Neytcheva M. Robust optimal multilevel preconditioners for non-conforming finite element systems. *Numer. Lin. Alg. Appl.*, 2005; **12**(5-6):495–514.

[17] Brezzi F, Cockburn B, Marini LD, Süli E. Stabilization mechanisms in discontinuous Galerkin finite element methods. *Comput. Methods Appl. Mech. Engrg.*, 2006; **195**:3293–3310.

[18] Brezzi F, Fortin M. *Mixed and Hybrid Finite Element Methods*. Springer-Verlag, Berlin, 1991.

[19] Carstensen C, Bartels S, Klose R. An experimental survey of a posteriori Courant finite element error control for the Poisson equation. *Adv. Comput. Math.*, 2001; **15**: 79–106.

[20] Carstensen C, Funken SA. Constants in Clément-interpolation error and residual based a posteriori error estimates in finite element methods. *East West J. Numer. Math.*, 2000; **8**(3): 153–175.

[21] Eijkhout V, Vassilevski PS. The role of the strengthened Cauchy-Bunyakowski-Schwarz inequality in multilevel methods. *SIAM Review,* 1991; **33**:405–419.

[22] Epshteyn Y, Rivière B. Estimation of penalty parameters for symmetric interior penalty Galerkin methods. *J. Comput. Appl. Math.*, 2007; **206**:843–872.

[23] Ern A, Stephansen AF, Vohralík M. Improved energy norm a posteriori error estimation based on flux reconstruction for discontinuous Galerkin methods. *SIAM J. Numer. Anal.*, 2007; submitted for publication.

[24] Georgiev I, Kraus J, Margenov S. Multilevel preconditioning of rotated bilinear non-conforming FEM problems. *Comput. Math. Appl.*, 2008; **55**:2280–2294.
[25] Gockenbach MS. *Understanding and implementing the finite element method*. SIAM, 2006.
[26] Hiptmair R. Multigrid method for $H(\mathrm{div})$ in three dimensions. *Electronic Transactions in Numerical Analysis*, 1997; **6**:133–152.
[27] Hiptmair R. Canonical construction of finite elements. *Math. Comp.*, 1999; **68**:1325–1346.
[28] Houston P, Schötzau D, Wihler TP. Energy norm a posteriori error estimation of *hp*-adaptive discontinuous Galerkin methods for elliptic problems. *Math. Models Methods Appl. Sci.* 2007; **17**(1): 33–62.
[29] Karakashian OA, Pascal F. A posteriori error estimates for a discontinuous Galerkin approximation of second-order elliptic problems. *SIAM J. Numer. Anal.*, 2003; **41**(6): 2374–2399.
[30] Kim KY. A posteriori error analysis for locally conservative mixed methods. *Math. Comp.* 2007 **76**(257): 43–66.
[31] Kraus J. An algebraic preconditioning method for M-matrices: linear versus nonlinear multilevel iteration. *Numer. Lin. Alg. Appl.* 2002; **9**:599–618.
[32] Kraus J, Margenov S, Synka J. On the multilevel preconditioning of Crouzeix-Raviart elliptic problems. *Numer. Lin. Alg. Appl.*, 2008; **15**:395-416.
[33] Kraus J, Tomar SK. Multilevel preconditioning of two-dimensional elliptic problems discretized by a class of discontinuous Galerkin methods. *SIAM J. Sci. Comput.*, 2008; **30**:684–786.
[34] Kraus J, Tomar SK. A multilevel method for discontinuous Galerkin approximation of three-dimensional anisotropic elliptic problems. *Numer. Linear Algebra Appl.*, 2008; **15**(5):417–438.
[35] Lazarov R, Repin S, Tomar SK. Functional a posteriori error estimates for discontinuous Galerkin approximations of elliptic problems. *Numer. Methods Partial Differential Equations*, DOI:10.1002/num.20386.
[36] Neittaanmäki P, Repin S. *Reliable methods for computer simulation, Error control and a posteriori estimates. Studies in Mathematics and its Applications*, vol. 33. Elsevier Science B.V., Amsterdam, 2004.
[37] Notay Y. Robust parameter-free algebraic multilevel preconditioning. *Numer. Lin. Alg. Appl.*, 2002; **9**:409–428.
[38] Repin S. A posteriori error estimation for nonlinear variational problems by duality theory. *Zap. Nauchn. Sem. S.-Peterburg. Otdel. Mat. Inst. Steklov. (POMI)* 1997 (342); **243**(Kraev. Zadachi Mat. Fiz. i Smezh. Vopr. Teor. Funktsii. 28): 201–214.
[39] Repin S. A unified approach to a posteriori error estimation based on duality error majorants. *Math. Comput. Simulation* 1999; **50**(1-4): 305–321.
[40] Repin S. A posteriori error estimation for variational problems with uniformly convex functionals. *Math. Comp.* 2000; **69**(230): 481–500.
[41] Repin S. Two-sided estimates of deviation from exact solutions of uniformly elliptic equations. *Proceedings of the St. Petersburg Mathematical Society* 2003; **IX**, 143–171, Amer. Math. Soc. Transl. Ser. **2**, 209.
[42] Repin S. A posteriori error estimation methods for partial differential equations. In *Lectures on Advanced Computational Methods in Mechanics*, Radon Series Comp. Appl. Math., Kraus J, Langer U (eds). **1**, 161–226, Walter de Gruyter, Berlin, 2007.
[43] Repin S, Tomar SK. A posteriori error estimates for nonconforming approximation of elliptic problems based on Helmholtz type decomposition of the error. *IMA J. Numer. Anal.*, submitted.
[44] Rivière B, Wheeler MF. A posteriori error estimates for a discontinuous Galerkin method applied to elliptic problems. *Comput. Math. Appl.* 2003; **46**: 141–164.
[45] Schwab C. *p- and hp- Finite Element Methods* Clarendon Press, Oxford, 1998.
[46] Saad Y. *Iterative Methods for Sparse Linear Systems.* PWS Publishing Company, Boston, 1996.
[47] Schneider R, Xu Y, Zhou A. An analysis of discontinuous Galerkin methods for elliptic problems. *Adv. Comput. Math.* 2006; **25**(1-3): 259–286.
[48] Tomar SK, Repin S. Efficient computable error bounds for discontinuous Galerkin approximations of elliptic problems. *J. Comput. Appl. Math.*, DOI:10.1016/j.cam.2008.08.015.
[49] Verfürth R. *A review of a posteriori error estimation and adaptive mesh refinement techniques.* Wiley-Teubner, Stuttgart, 1996.